

Single-photon emission of InAs/InP quantum dashes at 1.55 μm and temperatures up to 80 K

Ł. Dusanowski, M. Syperek, J. Misiewicz, A. Somers, S. Höfling, M. Kamp, J. P. Reithmaier, and G. Şek

Citation: *Applied Physics Letters* **108**, 163108 (2016); doi: 10.1063/1.4947448

View online: <http://dx.doi.org/10.1063/1.4947448>

View Table of Contents: <http://scitation.aip.org/content/aip/journal/apl/108/16?ver=pdfcov>

Published by the **AIP Publishing**

Articles you may be interested in

Single photon emission up to liquid nitrogen temperature from charged excitons confined in GaAs-based epitaxial nanostructures

Appl. Phys. Lett. **106**, 233107 (2015); 10.1063/1.4922455

Nanotemplate-directed InGaAs/GaAs single quantum dots: Toward addressable single photon emitter arrays

J. Vac. Sci. Technol. B **32**, 02C106 (2014); 10.1116/1.4863680

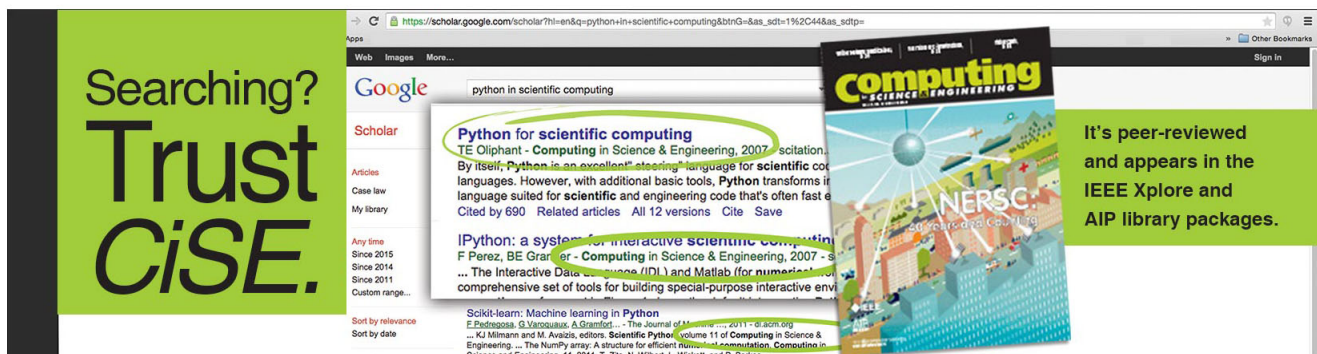
Long wavelength ($>1.55\mu\text{m}$) room temperature emission and anomalous structural properties of InAs/GaAs quantum dots obtained by conversion of In nanocrystals

Appl. Phys. Lett. **102**, 073103 (2013); 10.1063/1.4792700

Single quantum dot emission at telecom wavelengths from metamorphic InAs/InGaAs nanostructures grown on GaAs substrates

Appl. Phys. Lett. **98**, 173112 (2011); 10.1063/1.3584132

[APL Photonics](#)



Searching? Trust CiSE.

It's peer-reviewed and appears in the IEEE Xplore and AIP library packages.

python in scientific computing

Python for scientific computing
TE Oliphant - *Computing in Science & Engineering*, 2007 - scitation...
By itself, Python is an excellent scripting language for scientific computing languages. However, with additional basic tools, Python transforms into a language suited for scientific and engineering code that's often faster than C. Cited by 690 Related articles All 12 versions Cite Save

IPython: a system for interactive scientific computing
F. Perez, BE Granger - *Computing in Science & Engineering*, 2007 - sci...
... The Interactive Data Language (IDL) and Matlab (for numerical computing) comprehensive set of tools for building special-purpose interactive environments.

Scikit-learn: Machine learning in Python
E. Pedregosa, G. Varoquaux, A. Gramfort, ... - *The Journal of Machine Learning Research*, 2011 - 0.12618.org
... Ki. Mirmann and M. Avila, editors, *Scientific Python*, volume 11 of *Computing in Science & Engineering*, ... The NumPy array: A structure for efficient numerical computation, *Computing in Science and Engineering*, 11, 2011, T. Zito, N. Wilbert, L. Wiskott, and P. Berkes, ...

Single-photon emission of InAs/InP quantum dashes at 1.55 μm and temperatures up to 80 K

Ł. Dusanowski,^{1,a)} M. Syperek,¹ J. Misiewicz,¹ A. Somers,² S. Höfling,^{2,3} M. Kamp,² J. P. Reithmaier,^{2,4} and G. Sęk¹

¹Laboratory for Optical Spectroscopy of Nanostructures, Division of Experimental Physics, Faculty of Fundamental Problems of Technology, Wrocław University of Science and Technology, Wybrzeże Wyspiańskiego 27, 50-370 Wrocław, Poland

²Technische Physik, University of Würzburg, Wilhelm-Conrad-Röntgen-Research Center for Complex Material Systems, Am Hubland, D-97074 Würzburg, Germany

³School of Physics and Astronomy, University of St. Andrews, North Haugh, KY16 9SS St. Andrews, United Kingdom

⁴Institute of Nanostructure Technologies and Analytics (INA), CINSaT, University of Kassel, Heinrich-Plett-Str. 40, 34132 Kassel, Germany

(Received 21 March 2016; accepted 12 April 2016; published online 21 April 2016)

We report on single photon emission from a self-assembled InAs/InGaAlAs/InP quantum dash emitting at 1.55 μm at the elevated temperatures. The photon auto-correlation histograms of the emission from a charged exciton indicate clear antibunching dips with as-measured $g^{(2)}(0)$ values significantly below 0.5 recorded at temperatures up to 80 K. It proves that the charged exciton complex in a single quantum dash of the mature InP-based material system can act as a true single photon source up to at least liquid nitrogen temperature. This demonstrates the huge potential of InAs on InP nanostructures as the non-classical light emitters for long-distance fiber-based secure communication technologies. *Published by AIP Publishing.* [<http://dx.doi.org/10.1063/1.4947448>]

Single photons, due to their low decoherence, high speed transmission, and many degrees of freedom, are actually one of the most promising qubit implementations for the transmission of quantum information. Manipulation of single photons already allowed for the demonstration of free space quantum key distribution,^{1,2} simple quantum algorithms,³ CNOT (controlled NOT) gates, and entanglement manipulation following integrated photonic circuits approach.^{4,5} Key elements of such systems are pure and efficient sources of single photons. It has been well established that the exciton complexes confined within a self-assembled semiconductor quantum dot (QD) can be a true highly reliable microscopic single photon source (SPS).^{6,7} Due to the ability of monolithic integration of QDs with today's semiconductor devices, it has become feasible to fabricate SPSs with extraordinary parameters, combining nearly perfect levels of photon purity and indistinguishability as well as high extraction efficiencies reaching at least 60%–70%.^{8,9} Such state-of-the-art technology is currently based on the GaAs material system, and so far, most progress has been made for nanostructures emitting photons with wavelengths shorter than 1 μm . Nevertheless, long distance fiber-based quantum information technologies demand SPSs operating at the lowest loss telecommunication wavelengths at around 1.3 and 1.55 μm . Telecommunication wavelength emission can be achieved in GaAs system by combining InAs QDs with an additional InGaAs strain relaxation layer to increase the emission wavelength up to 1.3^{1,10–12} and even 1.55 μm .¹³ Following this approach, single photon emission has been demonstrated up to 1.3 μm ,^{1,11} which allowed for successful

quantum key distribution over 35 km using standard optical fibers at elevated temperatures.¹

An alternative technology, essential for the fabrication of structures at telecommunication wavelengths, is based on the InAs/InP material system. QDs in such a material system have been already shown to be efficient and pure single photon emitters at wavelengths including both the second^{14–16} and the third^{17–21} telecom band windows. High extraction efficiencies up to 46% (Ref. 16) and Purcell enhancement of the spontaneous emission rate as large as 5²⁰ have been already reported by successfully embedding InAs/InP QDs into different kinds of optical resonator structures including photonic crystal^{16,20} and micropillar²² cavities or optical horn structures.¹⁷ Only recently, 120 km range single photon quantum key distribution was demonstrated based on the InAs/InP quantum dots with the second order correlation function at the zero delay reaching values as low as 0.0051.²¹ Moreover, InAs/InP QDs embedded into photonic crystal cavities allowed for the first demonstration of on-demand 1.3 μm wavelength single photons with indistinguishabilities of 0.18 probed by two-photon interference measurements.¹⁶

In this letter, we investigate InAs/InGaAlAs/InP quantum dashes (QDashes), i.e., nanostructures which are strongly elongated in one of the in-plane directions, as potential telecom wavelength single photon emitters being able to operate at elevated temperatures. We report on the single-photon emission at a temperature of 80 K from a charged exciton complex emitting at around 1.55 μm . The charged character of this complex is revealed by polarization-resolved photoluminescence measurements, in compliance with our previous studies.¹⁹ Experiments have been performed on charged exciton emission since the lack of the

^{a)}Author to whom correspondence should be addressed. Electronic mail: lukasz.dusanowski@pwr.edu.pl

fine structure splitting of the charged exciton results in higher single-photon emission repetition rates compared to the neutral exciton ones.²³ By performing systematic studies of photoluminescence and photon emission statistics spectroscopy as a function of temperature, we demonstrate that such kind of nanostructures can be considered as a promising telecommunication C-band single photon source operating at liquid nitrogen temperatures. Furthermore, it is an important step towards thermoelectrically cooled telecom-band QDash-based SPSs, which should be achievable after further structure optimizations leading to increased quantum efficiencies and decreased thermal losses via the band structure and confinement engineering.²⁴

In Ref. 25, the influence of changing the population of phonons (via increasing temperature) on the exciton decoherence was studied both theoretically and experimentally in case of strongly asymmetric InAs/InP nanostructures. It was shown that the structural geometry has a major influence on the exciton-acoustic-phonon coupling strength. For strongly elongated nanostructures such as QDashes, the influence of the phonon-related decoherence is expected to be significantly weaker in comparison to typical QDs, but it cannot be entirely neglected and dominates the emission spectra above 100 K. Moreover, the theoretical studies performed for QDashes with lengths larger than 150 nm predict a weak decoherence even above 200 K.²⁶ These results suggest that photons emitted from the exciton complexes confined within InAs/InP QDashes should be much more robust against acoustic-phonons impact in comparison to more symmetric systems, which promises that QDashes might be well suited as telecom single photon sources operating at the elevated temperatures. In this letter, we make the first step in this direction and verify if indeed InAs/InP QDash nanostructures are able to generate the single photons at temperatures reaching at least the practical limit of cooling by liquid nitrogen cooling (~ 77 K).

The investigated sample was grown in an EIKO gas source molecular-beam epitaxy system on an S-doped InP(001) substrate. The layer sequence starts from a 200 nm-thick $\text{In}_{0.53}\text{Ga}_{0.23}\text{Al}_{0.24}\text{As}$ layer lattice matched to InP, which was grown on the substrate at 500 °C. In order to form QDashes in a self-assembled way, an InAs layer with a nominal thickness of 1.3 nm was deposited at 470 °C, out of which QDash structures on a wetting layer were formed. The QDashes were covered by a 100 nm-thick $\text{In}_{0.53}\text{Ga}_{0.23}\text{Al}_{0.24}\text{As}$ layer and subsequently capped with a 10 nm-thick layer of InP. Due to the atom's surface diffusion coefficient anisotropy, the epitaxially formed nanostructures are significantly elongated in one of the in-plane directions (preferentially the direction $[1\bar{1}0]$).²⁷ The typical lateral dimensions of QDashes under this study are about 20 nm in width and between 50 and hundreds of nanometers in length, whereas their height is approximately 3.5 nm.²⁸ Since the planar density of QDashes is rather high $\sim 5 \times 10^{10} \text{ cm}^{-2}$, a combination of electron beam lithography and etching techniques has been used to produce mesa structures with different sizes down to $0.125 \mu\text{m}^2$ ($500 \times 250 \text{ nm}^2$) in order to resolve the emission from single QDashes in an inhomogeneous ensemble.

For all the experiments, the sample was kept in a liquid-helium continuous-flow cryostat equipped with a heating wire attached to a proportional–integral–derivative temperature regulator loop for the sample temperature control. Spatially resolved photoluminescence spectroscopy and photon autocorrelation statistic measurements have been performed using a micro-photoluminescence (μPL) setup providing a spatial resolution on the order of a single μm and a spectral resolution of approx. $100 \mu\text{eV}$. The sample was excited with the 787 nm line of a continuous-wave (cw) semiconductor diode laser. The emission intensity of the isolated spectral lines has been detected by a liquid nitrogen-cooled InGaAs-based linear array detector combined with a 0.3 m focal length single grating monochromator. The degree of linear polarization (DOLP) has been measured by rotating a half-wave plate inserted in front of a linear polarizer placed at the monochromator entrance slit. Photon auto-correlation experiments were conducted with a Hanbury Brown and Twiss (HBT) setup. In this case, two short focal length monochromators with approx. 0.1 nm spectral resolution were used as spectral filters for the selected wavelengths corresponding to the charged exciton emission. Each of the monochromator outputs was equipped with a fiber-coupled NbN superconducting single-photon detector with $\sim 15\%$ quantum efficiency and ~ 10 dark counts/s at $1.55 \mu\text{m}$. The photon correlation statistics was acquired by a multichannel picosecond event timer. The overall temporal resolution of the system was ~ 80 ps.

Figure 1(a) shows the low temperature ($T = 5$ K) μPL spectra revealing a dominant emission line named charged exciton (CX) from a QDash enclosed within a mesa structure of $500 \times 250 \text{ nm}^2$ size. The spectrum was recorded under an excitation power of $\sim 4 \mu\text{W}$ (measured outside the cryostat). The CX line is centered at 0.8072 eV. The intensity of this CX line as a function of excitation power exhibits a close to linear dependence before saturating at an excitation power of $\sim 10 \mu\text{W}$ (inset in Fig. 1). This suggests neutral or charged exciton complex emission. Fig. 1(b) presents the spectral evolution of the CX line as a function of the linear

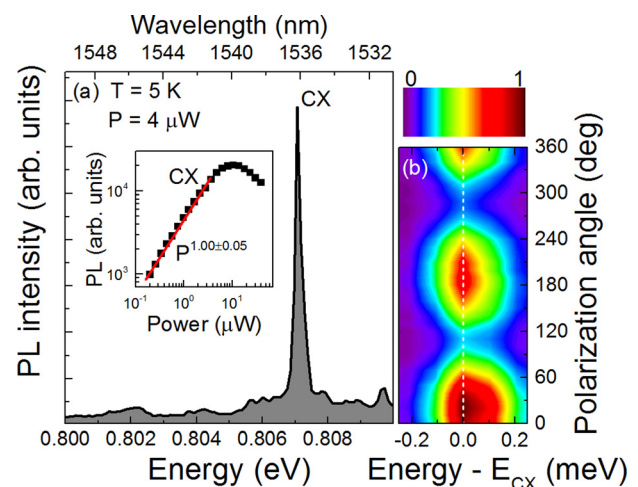


FIG. 1. (a) Low temperature (5 K) microphotoluminescence spectra from a charged exciton (CX) confined in an InAs/InP quantum dash excited cw at 787 nm. Inset: excitation power dependence of the CX peak intensity in a log-log scale. (b) Polarization resolved microphotoluminescence spectral map for CX emission.

polarization angle. The CX line energy reveals no polarization dependence within our setup resolution, indicating a charged character of CX line.¹⁹ In contrast to our previous results,^{19,29} we were not able to find any other exciton complexes originating from the same QDash. The nearest two neighboring emission lines visible above the CX energy at a distance of 2.8 and 4.3 meV (Fig. 2) are attributed to the emission of excitons from other individual QDashes, since the cross-correlation measurements did not reveal any mutual time dependencies. The CX line emission is significantly polarized with the degree of linear polarization (DOLP) of $\sim 60\%$ along the elongation axis. Such a high value of DOLP can be attributed to the combination of valence-band mixing effect being an intrinsic property of QDashes,^{30,31} and rectangular shape of a mesa structure, the geometry of which causes an enhancement of coupling between the quantum emitter and the optical field mode of a certain polarization.³²

In Figure 2, the temperature dependence of the μ PL spectrum of a single InAs/InP QDash from a $500 \times 250 \text{ nm}^2$ mesa is presented. For clarity, each spectrum has been normalized to the maximum of intensity. The line identified as a charged exciton CX can be easily followed in the entire temperature range. The graph shows a considerable and natural redshift of the luminescence peaks due to the band gap shrinkage (Fig. 3(b)) with increasing temperature. At a temperature of 80 K, the CX line energy is shifted by $\sim 6.2 \text{ meV}$

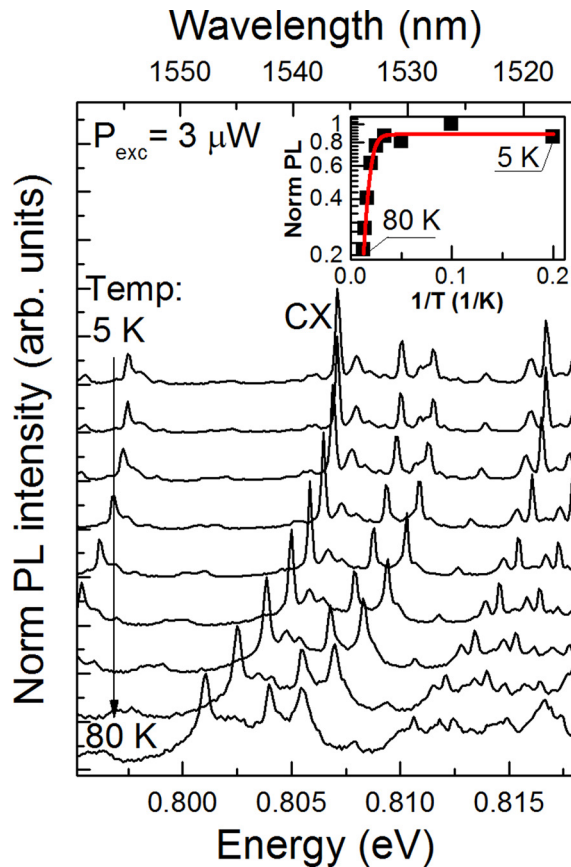


FIG. 2. (a) Temperature dependence of the PL spectra (normalized to maximum intensity) from a single mesa structure with InAs/InP QDashes in the range of 5–80 K recorded at the excitation power equal to $3 \mu\text{W}$. Inset: inverse temperature dependence of the intensity of the CX line photoluminescence. The solid line is a fit to the data yielding an activation energy of 20 meV.

with respect to low temperature spectra, allowing for the generation of $\sim 1548 \text{ nm}$ photons. At low temperatures of 5–30 K, the CX peak exhibits a Gaussian profile with a line-width of $\sim 0.2 \text{ meV}$, indicating the inhomogeneous impact of the environment on the QDash emission.³³ With increasing temperature sidebands appear, due to the coupling of the CX complex to acoustic phonons.²⁵ The temperature dependence of the CX emission line full width at half-maximum (FWHM) is presented in Fig. 3(a). The spectral linewidth increases with temperature, eventually broadening to $\sim 0.67 \text{ meV}$ at 80 K. It resembles a typical behavior predicted for a quantum dash exciton with a reduced phonon coupling strength due to the enlarged and anisotropic wave-function extension.²⁵ The inset in Fig. 2 presents the μ PL signal of the CX line plotted versus inverse temperature. The intensity of the CX line drops fivefold when the temperature is increased from 5 up to 80 K. This data was fitted by the Arrhenius formula (solid line) whereby the thermal quenching activation energy equal to $\sim 20 \text{ meV}$ was obtained. Such a value of activation energy may be associated with electrons escaping from the QDashes directly to the wetting layer.²⁴

The second order photon auto-correlation functions $g^{(2)}(\tau)$ of this CX emission have been recorded under cw excitation for various temperatures. In Figures 4(a)–4(d), the auto-correlation histograms for the charged exciton line are displayed for temperatures of 5, 30, 55, and 80 K, correspondingly. The excitation power used for these measurements was kept around $\sim 3\text{--}6 \mu\text{W}$ (depending on the temperature), well below the saturation power of the CX emission ($\sim 10 \mu\text{W}$). The excitation power has been increased slightly with temperature, which allowed compensating the reduction of the photon count rate due to the thermal quenching. All the recorded $g^{(2)}(\tau)$ functions show the clear photon antibunching dips at the zero time delay with $g^{(2)}(0)$ values significantly below the 0.5 limit. The low temperature histograms (up to 30 K) show $g^{(2)}(0)$ values around $\sim 0.18\text{--}0.19$. Non-zero $g^{(2)}(0)$ values are most likely due to the combination of the system background counts, large time bin (256 ps), and limited time resolution of the HBT setup

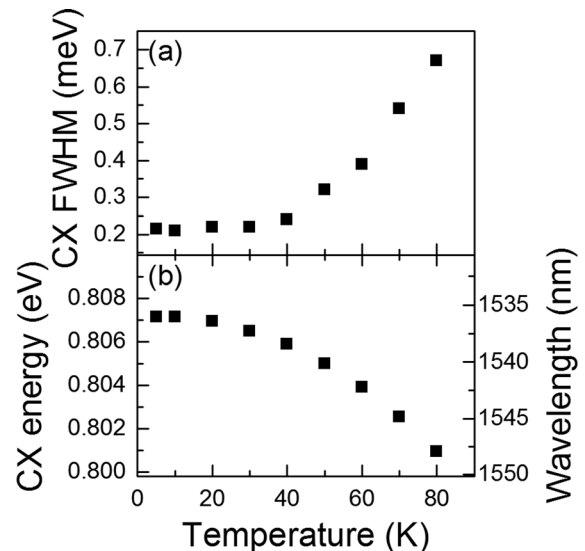


FIG. 3. (a) Temperature dependence of CX line full width at half-maximum. (b) Temperature dependence of CX energy.

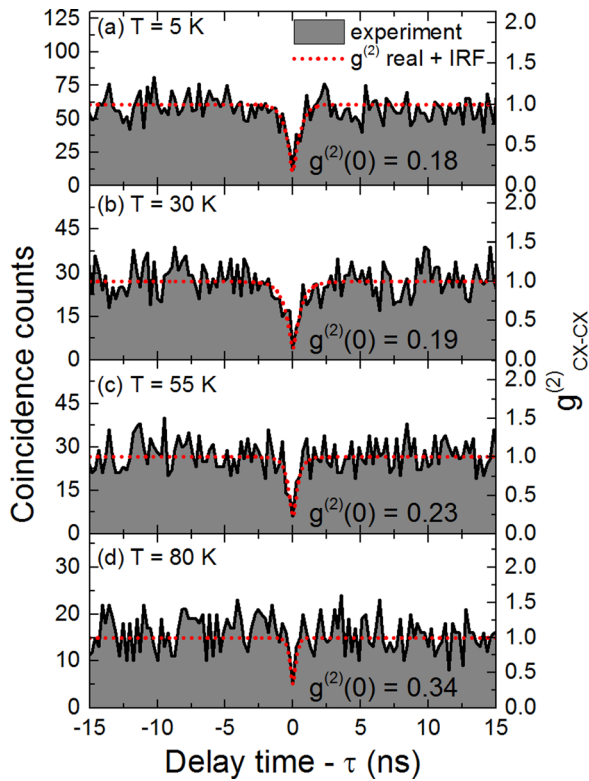


FIG. 4. Coincidence counts histograms recorded at temperatures 5 K (a), 30 K (b), 55 K (c), and 80 K (d) from CX emission. The solid line with the shaded area presents the raw experimental data and the red dotted line presents the fit of experimental data using the second order correlation function $g^{(2)}(t)$ convoluted with the instrumental response function (IRF). Raw values of $g^{(2)}(0)$ are obtained without any data post-processing. A clear antibunching dip with $g^{(2)}(0) < 0.5$ is observed in all cases.

(~ 80 ps). By performing the data fitting with a standard second order correlation function $g_R^{(2)}(\tau) = 1 - (1 - g_R^{(2)}(\tau = 0))\exp(-\frac{|\tau|}{\tau_f})$ convoluted with the system instrumental response function (IRF) in the form of $\exp(-\frac{|\tau|}{\tau_{IRF}})$, where τ_{IRF} is the setup time resolution (80 ps), the resulting $g_R^{(2)}(0)$ for both histograms reaches almost zero value (see the dashed lines in Fig. 4). The antibunching time constant τ_f was determined to be 0.48 and 0.46 at the temperatures of 5 and 30 K, respectively. Such small values of τ_f in respect to predicted radiative lifetimes (1–2 ns (Ref. 29)) suggest that the CX occupation changes and therefore also $g^{(2)}(\tau)$ build-ups are limited mainly by high photoexcitation rates.³⁴ With increasing temperature, $g^{(2)}(0)$ values increase from ~ 0.23 at 55 K to ~ 0.34 at 80 K (Figs. 4(c) and 4(d)). The observed decrease of the single photon emission purity may be attributed to the background photons emitted from the neighboring QDashes which become pronounced at higher temperatures due to the acoustic-phonon-related sidebands (80 K spectra in Fig. 2). To estimate the background influence on the $g^{(2)}(0)$ value, we performed a rough signal (S) to background (B) ratio estimation $\rho = S/(S + B)$, where S was taken as the CX peak intensity and B as a means of the low and high energy background intensities of the CX peak. Assuming a Poissonian background character, the measured $g^{(2)}(0)$ value should be increased by $1 - \rho^2$ factor.³⁵ For 55 K (80 K) temperature, ρ was determined to be 0.89 (0.84)

resulting in a $g_B^{(2)}(0) = 1 - \rho^2$ value of ~ 0.21 (~ 0.29). The obtained values of $g_B^{(2)}(0)$ are slightly overestimated taking into account the additional effect of IRF (for 55 K: $0.18 + 0.21 > 0.23$), which may be a result of rather simplified background counts' determination method. Despite this inconsistency, such rough estimation of the background points out at a non-negligible influence of neighboring QDashes on photon statistics at elevated temperatures. This effect may be suppressed in future by better separation of QDashes, for example, by modifying the sample growth mode in order to reduce the nanostructures' surface densities.

In conclusion, we have investigated the temperature dependence of photon emission from a single InAs/InGaAlAs/InP quantum dash emitting at $1.55 \mu\text{m}$ by μPL and photon-correlation spectroscopy. Single-photon emission has been verified under cw non-resonant optical excitation on the charged exciton emission. A charged character of the exciton complex has been confirmed by the power-dependent and polarization resolved μPL . We were able to observe the single photon emission up to the temperature of 80 K with a raw value of $g^{(2)}(0)$ equal to ~ 0.34 , proving that the investigated structures can be considered as true single photon emitters able to operate at telecommunication wavelengths at liquid nitrogen temperatures. This is a promising result and an important milestone with respect to the practical application of InAs on InP epitaxial nanostructures in quantum information technologies.

This research was supported by the National Science Center of Poland within Grant No. 2011/02/A/ST3/00152.

- ¹P. M. Intallura, M. B. Ward, O. Z. Karimov, Z. L. Yuan, P. See, A. J. Shields, P. Atkinson, and D. A. Ritchie, *Appl. Phys. Lett.* **91**, 161103 (2007).
- ²M. Rau, T. Heindel, S. Unsleber, T. Braun, J. Fischer, S. Frick, S. Nauerth, C. Schneider, G. Vest, S. Reitzenstein, M. Kamp, A. Forchel, S. Höfling, and H. Weinfurter, *New J. Phys.* **16**, 043003 (2014).
- ³B. P. Lanyon, T. J. Weinhold, N. K. Langford, M. Barbieri, D. F. V. James, A. Gilchrist, and A. G. White, *Phys. Rev. Lett.* **99**, 250505 (2007).
- ⁴H. Jin, F. M. Liu, P. Xu, J. L. Xia, M. L. Zhong, Y. Yuan, J. W. Zhou, Y. X. Gong, W. Wang, and S. N. Zhu, *Phys. Rev. Lett.* **113**, 103601 (2014).
- ⁵J. Wang, A. Santamato, P. Jiang, D. Bonneau, E. Engin, J. W. Silverstone, M. Lerner, J. Beetz, M. Kamp, S. Höfling, M. G. Tanner, C. M. Natarajan, R. H. Hadfield, S. N. Dorenbos, V. Zwiller, J. L. O'Brien, and M. G. Thompson, *Opt. Commun.* **327**, 49 (2014).
- ⁶S. Buckley, K. Rivoire, and J. Vučković, *Rep. Prog. Phys.* **75**, 126503 (2012).
- ⁷P. Michler, A. Kiraz, C. Becher, W. V. Schoenfeld, P. M. Petroff, L. Zhang, E. Hu, and A. Imamoglu, *Science* **290**, 2282 (2000).
- ⁸X. Ding, Y. He, Z.-C. Duan, N. Gregersen, M.-C. Chen, S. Unsleber, S. Maier, C. Schneider, M. Kamp, S. Höfling, C.-Y. Lu, and J.-W. Pan, *Phys. Rev. Lett.* **116**, 020401 (2016).
- ⁹N. Somaschi, V. Giesz, L. De Santis, J. C. Loredó, M. P. Almeida, and G. Hornecker *et al.*, "Near-optimal single-photon sources in the solid state," *Nat. Photonics* (published online).
- ¹⁰B. Alloing, C. Zinoni, V. Zwiller, L. H. Li, C. Monat, M. Gobet, G. Buchs, A. Fiore, E. Pelucchi, and E. Kapon, *Appl. Phys. Lett.* **86**, 101908 (2005).
- ¹¹M. B. Ward, O. Z. Karimov, D. C. Unitt, Z. L. Yuan, P. See, D. G. Gevaux, A. J. Shields, P. Atkinson, and D. A. Ritchie, *Appl. Phys. Lett.* **86**, 201111 (2005).
- ¹²M. Strauss, S. Höfling, and A. Forchel, *Nanotechnology* **20**, 505601 (2009).
- ¹³E. S. Semenova, R. Hostein, G. Patriarche, O. Manguin, L. Largeau, I. Robert-Philip, A. Beveratos, and A. Lemaître, *J. Appl. Phys.* **103**, 103533 (2008).

- ¹⁴K. Takemoto, Y. Sakuma, S. Hirose, T. Usuki, N. Yokoyama, T. Miyazawa, M. Takatsu, and Y. Arakawa, *Jpn. J. Appl. Phys., Part 2* **43**, L993 (2004).
- ¹⁵D. Elvira, R. Hostein, B. Fain, L. Monniello, A. Michon, G. Beaudoin, R. Braive, I. Robert-Philip, I. Abram, I. Sagnes, and A. Beveratos, *Phys. Rev. B* **84**, 195302 (2011).
- ¹⁶J. Kim, T. Cai, C. J. K. Richardson, R. P. Leavitt, and E. Waks, e-print [arXiv:1511.05617](https://arxiv.org/abs/1511.05617).
- ¹⁷K. Takemoto, M. Takatsu, S. Hirose, N. Yokoyama, Y. Sakuma, T. Usuki, T. Miyazawa, and Y. Arakawa, *J. Appl. Phys.* **101**, 081720 (2007).
- ¹⁸M. Benyoucef, M. Yacob, J. P. Reithmaier, J. Kettler, and P. Michler, *Appl. Phys. Lett.* **103**, 162101 (2013).
- ¹⁹Ł. Dusanowski, M. Syperek, P. Mrowiński, W. Rudno-Rudziński, J. Misiewicz, A. Somers, S. Höfling, M. Kamp, J. P. Reithmaier, and G. Sek, *Appl. Phys. Lett.* **105**, 021909 (2014).
- ²⁰M. D. Birowosuto, H. Sumikura, S. Matsuo, H. Taniyama, P. J. van Veldhoven, R. Nötzel, and M. Notomi, *Sci. Rep.* **2**, 321 (2012).
- ²¹K. Takemoto, Y. Nambu, T. Miyazawa, Y. Sakuma, T. Yamamoto, S. Yorozu, and Y. Arakawa, *Sci. Rep.* **5**, 14383 (2015).
- ²²S. Frederick, D. Dalacu, D. Poitras, G. C. Aers, P. J. Poole, J. Lefebvre, D. Chithrani, and R. L. Williams, *Microelectron. J.* **36**, 197 (2005).
- ²³S. Strauf, N. G. Stoltz, M. T. Rakher, L. A. Coldren, P. M. Petroff, and D. Bouwmeester, *Nat. Photonics* **1**, 704 (2007).
- ²⁴P. Podemski, R. Kudrawiec, J. Misiewicz, A. Somers, R. Schwertberger, J. P. Reithmaier, and A. Forchel, *Appl. Phys. Lett.* **89**, 151902 (2006).
- ²⁵Ł. Dusanowski, A. Musiał, A. Maryński, P. Mrowiński, J. Andrzejewski, P. Machnikowski, J. Misiewicz, A. Somers, S. Höfling, J. P. Reithmaier, and G. Sek, *Phys. Rev. B* **90**, 125424 (2014).
- ²⁶Ł. Dusanowski, A. Musiał, G. Sek, and P. Machnikowski, *Acta Phys. Pol., A* **124**, 813 (2013).
- ²⁷J. Brault, M. Gendry, G. Grenet, G. Hollinger, Y. Desières, and T. Benyattou, *Appl. Phys. Lett.* **73**, 2932 (1998).
- ²⁸A. Sauerwald, T. Kümmell, G. Bacher, A. Somers, R. Schwertberger, J. P. Reithmaier, and A. Forchel, *Appl. Phys. Lett.* **86**, 253112 (2005).
- ²⁹Ł. Dusanowski, M. Syperek, W. Rudno-Rudziński, P. Mrowiński, G. Sek, J. Misiewicz, A. Somers, J. P. Reithmaier, S. Höfling, and A. Forchel, *Appl. Phys. Lett.* **103**, 253113 (2013).
- ³⁰P. Kaczmarkiewicz and P. Machnikowski, *Semicond. Sci. Technol.* **27**, 105012 (2012).
- ³¹A. Musiał, P. Kaczmarkiewicz, G. Sek, P. Podemski, P. Machnikowski, J. Misiewicz, S. Hein, S. Höfling, and A. Forchel, *Phys. Rev. B* **85**, 035314 (2012).
- ³²P. Mrowiński, K. Tarnowski, J. Olszewski, A. Somers, M. Kamp, S. Höfling, J. P. Reithmaier, W. Urbańczyk, J. Misiewicz, P. Machnikowski, and G. Sek, *Acta Phys. Pol., A* **129**, A48 (2016).
- ³³J. Seufert, R. Weigand, G. Bacher, T. Kümmell, A. Forchel, K. Leonardi, and D. Hommel, *Appl. Phys. Lett.* **76**, 1872 (2000).
- ³⁴D. Regelman, U. Mizrahi, D. Gershoni, E. Ehrenfreund, W. Schoenfeld, and P. Petroff, *Phys. Rev. Lett.* **87**, 257401 (2001).
- ³⁵K. Sebald, P. Michler, T. Passow, D. Hommel, G. Bacher, and A. Forchel, *Appl. Phys. Lett.* **81**, 2920 (2002).